

## *Saccharomyces cerevisiae* Grx6 and Grx7 Are Monothiol Glutaredoxins Associated with the Early Secretory Pathway<sup>∇†</sup>

Alicia Izquierdo,<sup>1</sup> Celia Casas,<sup>1</sup> Ulrich Mühlenhoff,<sup>2</sup> Christopher Horst Lillig,<sup>2</sup> and Enrique Herrero<sup>1\*</sup>

*Departament de Ciències Mèdiques Bàsiques, IRBLleida, Universitat de Lleida, 25008-Lleida, Spain,<sup>1</sup> and Institut für Zytobiologie und Zytopathologie, Philipps Universität Marburg, Marburg D-35033, Germany<sup>2</sup>*

Received 14 April 2008/Accepted 15 May 2008

***Saccharomyces cerevisiae* Grx6 and Grx7 are two monothiol glutaredoxins whose active-site sequences (CSYS and CPYS, respectively) are reminiscent of the CPYC active-site sequence of classical dithiol glutaredoxins. Both proteins contain an N-terminal transmembrane domain which is responsible for their association to membranes of the early secretory pathway vesicles, facing the luminal side. Thus, Grx6 localizes at the endoplasmic reticulum and Golgi compartments, while Grx7 is mostly at the Golgi. Expression of *GRX6* is modestly upregulated by several stresses (calcium, sodium, and peroxides) in a manner dependent on the Crz1-calciurein pathway. Some of these stresses also upregulate *GRX7* expression under the control of the Msn2/4 transcription factor. The N glycosylation inhibitor tunicamycin induces the expression of both genes along with protein accumulation. Mutants lacking both glutaredoxins display reduced sensitivity to tunicamycin, although the drug is still able to manifest its inhibitory effect on a reporter glycoprotein. Grx6 and Grx7 have measurable oxidoreductase activity *in vivo*, which is increased in the presence of tunicamycin. Both glutaredoxins could be responsible for the regulation of the sulfhydryl oxidative state at the oxidant conditions of the early secretory pathway vesicles. However, the differences in location and expression responses against stresses suggest that their functions are not totally overlapping.**

Glutaredoxins (Grxs) are thiol oxidoreductases that catalyze the reduction of intra- and intermolecular disulfides using reduced glutathione (GSH) as the electron donor (29). They carry out a variety of physiological functions (reviewed in references 19 and 28), which include ribonucleotide reductase and 3'-phosphoadenylylsulfate reductase activation, ascorbate reduction, and regulation of the DNA binding activity of nuclear factors, among others. Classical (dithiol) Grxs contain a CPY/FC active-site motif, and they operate through a mechanism of action that involves both cysteine residues for reducing protein disulfides. However, only the most N-terminal cysteine of the active site is required for deglutathionylation of mixed disulfides between glutathione and protein cysteines (6). Dithiol Grx activity is usually measured through its ability to reduce the mixed disulfide formed between GSH and one mercaptoethanol moiety of the  $\beta$ -hydroxyethyl disulfide (HEDS) substrate (29). More recently, another Grx subfamily containing the active-site CGFS motif has been described. For this reason, they have been named monothiol Grxs (reviewed in reference 28). Monothiol Grxs do not display activity in the HEDS assay, and members of this subfamily are present in organisms from prokaryotes to higher eukaryotes. In addition, plants may have other Grx subfamilies with conserved motifs different from those characteristic of the dithiol and monothiol Grxs (56).

*Saccharomyces cerevisiae* provides an example of the diver-

sity of locations and functions for Grxs. This yeast contains two dithiol Grxs (Grx1 and Grx2), which are cytosolic (38), but a minor part of Grx2 is also present in mitochondria (51). The physiological function of Grx1 and Grx2 is not clearly established, although yeast cells show some hypersensitivity to oxidants in their absence (13, 38). In addition, *S. cerevisiae* has three monothiol Grxs (54). Two of them (Grx3 and Grx4) are nucleocytoplasmic (37, 43) and are involved in iron homeostasis, probably through the regulation of the location of Aft1, which is a transcription factor controlling the expression of genes implicated in the assimilation of iron in yeast cells (48, 52). The third monothiol Grx (Grx5) is at the mitochondrial matrix and participates in the synthesis of Fe/S clusters (35, 45, 55). In eukaryotic microorganisms and animals, synthesis of Fe/S clusters occurs mainly, if not exclusively, in mitochondria, while plant chloroplasts also contain machinery for Fe/S biogenesis (45). Homologues of Grx5 from bacteria (44), zebra fish (68), humans (44), and plants (10) can substitute for native Grx5 in the Fe/S synthesis function in yeast cells, supporting the functional conservation of Grx5 along the course of evolution. In accordance with this, the absence of Grx5 function in zebra fish and human cells results in pathologies associated with iron metabolism alterations (7, 68).

Some dithiol Grx molecules themselves may contain Fe/S clusters required for enzyme structure and activity. This is the case of human Grx2 (3, 32, 36) and poplar Grx C1 (57). Human Grx2 may act as a sensor of oxidative stress conditions through its Fe/S clusters, which would have a structural role (36). Several CGFS-type monothiol Grxs also contain Fe/S clusters, at least when purified from bacterial cells (50), although *in vivo* studies are required to confirm the physiological significance of these observations.

Recently, two additional Grxs in *S. cerevisiae*, named Grx6

\* Corresponding author. Mailing address: Departament de Ciències Mèdiques Bàsiques, Facultat de Medicina, Universitat de Lleida, Montserrat Roig 2, 25008 Lleida, Spain. Phone: (34) 973-702409. Fax: (34) 973-702426. E-mail: enric.herrero@cmb.udl.cat.

† Supplemental material for this article may be found at <http://ec.asm.org/>.

<sup>∇</sup> Published ahead of print on 23 May 2008.

TABLE 1. Strains used in this work

Strain	Relevant genotype	Comment(s)
W303-1A	<i>MATa ura3-1 ade2-1 leu2-3,112 trp1-1 his3-11,15</i>	Wild type
W303-1B	<i>MAT<math>\alpha</math> ura3-1 ade2-1 leu2-3,112 trp1-1 his3-11,15</i>	Wild type
Wmsn2msn4	W303-1A <i>msn2::HIS3 msn4::TRP1</i>	From F. Estruch
MML752	W303-1A <i>grx1::kanMX4 grx2::LEU2</i>	Reference 21
MML866	W303-1B <i>grx7::kanMX4</i>	<i>GRX7</i> disruption with <i>kanMX4</i> cassette
MML871	W303-1A <i>crz1::kanMX4</i>	Deletion region moved from BY4741; <i>crz1::kanMX4</i>
MML887	W303-1A <i>grx7::kanMX4</i>	<i>GRX7</i> disruption with <i>kanMX4</i> cassette
MML890	W303-1A <i>grx6::CaURA3</i>	<i>GRX6</i> disruption with <i>CaURA3</i> cassette
MML892	W303-1A <i>grx6::CaURA3 grx7::kanMX4</i>	From a cross, MML866 $\times$ MML890
MML897	W303-1A [pMM799( <i>GRX6-3HA</i> )]: <i>URA3</i>	Integration of pMM799 in W303-1A
MML949	W303-1A <i>GRX7-3HA::hphNT1</i>	Chromosomal <i>GRX7</i> tagged with 3HA using the <i>hphNT1</i> cassette
MML953	W303-1A <i>GRX6-3HA::hphNT1</i>	Chromosomal <i>GRX6</i> tagged with 3HA using the <i>hphNT1</i> cassette
MML999	W303-1A [pMM881( <i>GRX7-3HA</i> )]: <i>URA3</i>	Integration of pMM881 in W303-1A
MML1001	W303-1A [pMM799( <i>GRX6-3HA</i> )]: <i>URA3 OLE1::GFP</i>	<i>OLE1::GFP</i> construction moved from CYC243 (Vergés et al., 2007 [65]) into MML897
MML1003	W303-1A [pMM881( <i>GRX7-3HA</i> )]: <i>URA3 OLE1::GFP</i>	<i>OLE1::GFP</i> construction moved from CYC243 into MML999
MML1005	W303-1A; <i>OLE1::GFP</i> into W303-1A	<i>OLE1::GFP</i> construction moved from CYC243
MML1037	W303-1A [pMM894( <i>GRX6D3/40-3HA</i> )]: <i>URA3</i>	Integration of pMM894 in W303-1A
MML1039	W303-1A [pMM896( <i>GRX7D3/36-3HA</i> )]: <i>URA3</i>	Integration of pMM896 in W303-1A
CML128	<i>MATa ura3-52 leu2-3,112 trp1-1 his4</i>	Wild type; reference 20
CYC209	CML128 <i>tTA-LEU2 KAR2-6FLAG-kanMX4</i>	Reference 33, from M. Aldea
CYC211	CML128 <i>tTA-LEU2 SEC62-6FLAG-kanMX4</i>	Reference 33, from M. Aldea
MML1011	CYC209 <i>KAR2-6FLAG-kanMX4</i> [pMM881( <i>GRX7-3HA</i> )]: <i>URA3</i>	Integration of pMM881 into CYC209
MML1012	CYC211 <i>SEC62-6FLAG-kanMX4</i> [pMM881( <i>GRX7-3HA</i> )]: <i>URA3</i>	Integration of pMM881 into CYC211
MML1013	CYC209 <i>KAR2-6FLAG-kanMX4</i> [pMM799( <i>GRX6-3HA</i> )]: <i>URA3</i>	Integration of pMM799 into CYC209
MML1014	CYC211 <i>SEC62-6FLAG-kanMX4</i> [pMM799( <i>GRX6-3HA</i> )]: <i>URA3</i>	Integration of pMM799 into CYC211
BY4741	<i>MATa his3D1 leu2D0 met15D0 ura3D0</i>	Wild type
Y03792	BY4741 <i>pmt1::kanMX4</i>	From Euroscarf, deletion of <i>PMT1</i>
Y00385	BY4741 <i>pmt2::kanMX4</i>	From Euroscarf, deletion of <i>PMT2</i>
Y01618	BY4741 <i>pmt3::kanMX4</i>	From Euroscarf, deletion of <i>PMT3</i>
Y03790	BY4741 <i>pmt5::kanMX4</i>	From Euroscarf, deletion of <i>PMT5</i>
Y04829	BY4741 <i>pmt6::kanMX4</i>	From Euroscarf, deletion of <i>PMT6</i>
AN1-7D	<i>MAT<math>\alpha</math> ura3-52 trp1 leu2-3,112 sec18ts</i>	Reference 47
MML1010	AN1-7D [pMM799 ( <i>GRX6-3HA</i> )]: <i>URA3</i>	Integration of pMM799 into AN1-7D

and Grx7, have been described (39, 40). They contain CSYS and CPYS motifs, respectively, at their active sites. Therefore, they should be also defined as monothiol Grxs, although the primary sequences of their Grx modules are more similar to those of dithiol Grxs than to those of monothiol Grxs of the CGFS type (39, 40). In contrast to the latter, both Grx6 and Grx7 are active in the HEDS assay and, when purified from bacteria, Grx6 (but not Grx7) binds two Fe/S clusters which are required for tetramer formation. Detailed analysis of their primary sequences indicates that Grx6 and Grx7 contain a putative transmembrane (TM) domain at their N-terminal ends. This suggests that both of them may be membrane-associated Grxs and that their functions may be related to redox regulation in the oxidant conditions occurring in the secretory machinery compartments (8, 64). In this study, we describe the cellular location of Grx6 and Grx7, demonstrate their *in vivo* activity as Grxs, analyze their expression in different physiological conditions, and provide some evidence as to their possible functions. The results demonstrate that although Grx6 and Grx7 display significant structural and biochemical similarities, some differences exist between them concerning

cellular location, responses to stresses, and posttranslational modifications.

## MATERIALS AND METHODS

**Strains and growth conditions.** The *S. cerevisiae* strains employed in this work are described in Table 1. Cells were grown at 30°C unless stated otherwise, using yeast extract-peptone-dextrose (YEPD) medium (1% yeast extract, 2% peptone, 2% glucose) or SC medium (0.67% yeast nitrogen base, 2% glucose plus dropout mixture and auxotrophic requirements [60]). Specific supplements were omitted for selection of the corresponding plasmid-carrying cells. Cells were grown exponentially for at least 10 generations before samples were taken for analyses.

**Plasmid and strain construction.** Plasmids pMM799 and pMM881 are *S. cerevisiae* *URA3* integrative plasmids derived from YIplac211 (23), which contain, respectively, the *GRX6* and *GRX7* genes tagged at their 3' ends with the 3HA epitope sequence plus 814 (*GRX6*) or 750 (*GRX7*) nucleotides upstream from the respective translation initiation sites. Plasmid pMM894 derives from pMM799 by deletion from codon 3 to codon 40 (inclusive) of the *GRX6* coding region. Deletion was made using the ExSite method (67). Similarly, plasmid pMM896 derives from pMM881 by deletion from codon 3 to codon 36 of the *GRX7* coding region. Plasmids pMM892 (centromeric; *URA3*) and pMM866 (episomal; *URA3*) derive from YCplac33 and YEplac195, respectively (23), and contain a 3HA-tagged *GRX6* sequence with its own promoter region (as for pMM799). Plasmid pMM880 was obtained from pMM866 by mutating the codon for the C136 residue in *GRX6* for a serine codon by use of the ExSite method.

Plasmid pMM822 is a YEplac195 derivative which contains the *GRX6* open reading frame plus 814 nucleotides of the promoter region and 284 nucleotides downstream of the stop codon. Similarly, pMM763 derives from YEplac195 and contains the *GRX7* coding sequence plus 750 upstream and 364 downstream nucleotides.

Standard protocols were used for DNA manipulations and cell transformations. Single null mutants were obtained by using the short flanking homology approach after PCR amplification of the *kanMX4* (66) and the *CaURA3MX* (25) cassettes. Disruptions were confirmed by PCR analysis. Multiple mutants were obtained by crossing the parental mutant strains, followed by diploid sporulation, tetrad analysis, and selection of the mutant combinations (60). For *3HA* tagging of the coding terminus of the chromosomal copies of *GRX6* and *GRX7*, the pYM24 plasmid was employed, using the *hphNT1* cassette and selecting for hygromycin B resistance (31).

**Subcellular fractionation.** Crude membrane fractions were prepared after mechanical breakage of yeast cells in lysis buffer (0.1 M sorbitol, 50 mM potassium acetate, 20 mM HEPES, pH 7.5, 2 mM EDTA, 1 mM dithiothreitol plus protease inhibitors [2 mM phenylmethylsulfonyl fluoride, 0.2 mM tolylsulfonyl phenylalanyl chloromethyl ketone, 2  $\mu$ M pepstatin A]) on ice. Cells debris was removed by centrifugation ( $700 \times g$ , 5 min) and the supernatant was subjected to different treatments for protein extraction for 1 h at 0°C as follows: 0.5 M NaCl, 2.5 M urea, 0.1 M Na<sub>2</sub>CO<sub>3</sub> at pH 11.5, or 1% Triton X-100 plus 0.5 M NaCl. Subsequently, the samples were separated into supernatant and pellet fractions by centrifugation ( $100,000 \times g$ , 2 h) at 4°C.

Subcellular fractionation in 20 to 60% sucrose gradients was carried out in the presence of either 2 mM MgCl<sub>2</sub> or 10 mM EDTA. Essentially, cultured cells were centrifuged; washed in 50 mM Tris-HCl buffer, pH 7.5, plus 10 mM sodium azide and 10 mM potassium fluoride; and incubated for 20 min at 30°C in 50 mM Tris-HCl buffer, pH 7.5, plus 0.5% 2-mercaptoethanol. After the cells were spun, they were resuspended in protoplasting buffer (1.2 M sorbitol, 0.5 mM MgCl<sub>2</sub>, 40 mM HEPES, pH 7.5) plus Zymolyase 100T (2 mg per g of cells [dry weight]) and incubated at 30°C until protoplast formation was almost complete (usually about 30 min). Protoplasts were collected by centrifugation ( $2,500 \times g$ , 5 min) at 4°C and lysed by resuspension in STE10 buffer (10% sucrose, 10 mM Tris HCl, pH 7.5, 1 mM dithiothreitol, protease inhibitors, and either 2 mM MgCl<sub>2</sub> or 10 mM EDTA) followed by Dounce homogenization. Intact cells and large cell aggregates were removed by centrifugation at  $2,500 \times g$  for 2 min at 4°C. The resulting supernatant was applied to the respective sucrose gradient containing either MgCl<sub>2</sub> or EDTA, and the subsequent steps were as described in reference 53.

**Proteinase K protection assay.** Cells expressing epitope-tagged proteins were mechanically disrupted with glass beads in 0.7 M sorbitol in 50 mM Tris-HCl buffer, pH 7.5. After elimination of unbroken cells and cell aggregates by centrifugation ( $700 \times g$ , 5 min) at 4°C, the supernatant was left untreated or was treated with proteinase K (0.1 mg/ml) or with proteinase K plus 1% Triton X-100 for 20 min at 0°C. After the addition of phenylmethylsulfonyl fluoride (final concentration, 5 mM), proteins were precipitated with 15% trichloroacetic acid. Pellets were solubilized for sodium dodecyl sulfate-polyacrylamide gel electrophoresis and Western blot analyses.

**Western blotting.** Western blot analyses were done as described in reference 2. The following primary antibodies were employed: 12CA5 mouse monoclonal anti-hemagglutinin (HA) (dilution 1:2,500; Roche), M2 mouse monoclonal anti-FLAG (1:1,500; Sigma), 5C5 mouse monoclonal anti-Dpm1 (1:2,000; Molecular Probes), rabbit polyclonal anti-Emp47 (1:2,000 [59]), rabbit polyclonal anti-Hxk1 (1:5,000; USBiological), or 10A5 mouse monoclonal anti-carboxypeptidase Y (CPY) (1:500; Molecular Probes).

**Northern blotting.** RNA electrophoresis, probe labeling with digoxigenin, hybridization, and signal detection in a Lumi-Imager instrument (Roche Applied Science) were done as described previously (2). Gene probes were PCR generated from genomic DNA, using oligonucleotides designed to amplify internal open reading frame regions.

**Immunofluorescence microscopy.** Immunofluorescence colocalization of Grx6-HA or Grx7-HA proteins and the green fluorescent protein (GFP)-fused endoplasmic reticulum (ER) marker Ole1 was done as described in reference 65. 3F10 rat anti-HA (Roche) and Alexa555 goat anti-rat (Molecular Probes) antibodies were employed for signal detection. Colocalization of Grx6-HA or Grx7-HA and the Golgi marker Emp47 was done as described above, except that incubations were sequentially made with the anti-Emp47 antibody in the presence of 0.1% Triton X-100 followed by the anti-HA antibody without detergent. Emp47 signal was detected with rabbit anti-Emp47 (59) and Alexa485 goat anti-rabbit (Molecular Probes) antibodies.

**Determination of thiol oxidoreductase activity.** Thiol oxidoreductase (glutaredoxin) activity was measured with HEDS as the substrate, as described previously (29), using extracts from exponential cells after mechanical disruption and the

elimination of unbroken cells and aggregates by centrifugation ( $700 \times g$ , 5 min) at 4°C.

**In vivo labeling with <sup>55</sup>Fe and protein immunoprecipitation.** In vivo labeling of yeast cells with <sup>55</sup>FeCl and analysis of iron binding to HA-tagged proteins by immunoprecipitation and scintillation counting was done as described in reference 42. F7 mouse monoclonal anti-HA antibodies (Santa Cruz) were used for immunoprecipitations.

## RESULTS

**Putative membrane-associated monothiol Grxs exist in diverse fungal species.** *S. cerevisiae* Grx6 and Grx7 proteins have a Grx module with an N-terminal extension that includes a putative TM domain (see Fig. S1A in the supplemental material). The Grx module displays a high degree of homology with *S. cerevisiae* Grx1 and Grx2 and with other dithiol Grxs (39, 40). However, the active-site sequences of both monothiol Grxs (CSYS for Grx6 and CPYS for Grx7) differ from the active sites of dithiol Grxs. A BLAST analysis based on the Grx modules of Grx6 and Grx7 revealed that homologues of these two proteins exist only in fungi, some plants, and worms. They share the following sequence, which includes the active site: I/VF/YSKS/TXCP/SXS. Two subtypes can be established based on the alternative amino acid (S or P) adjacent to the active-site cysteine (see Table S1 in the supplemental material). The *Saccharomyces sensu stricto* species contain one member of each subtype, while other organisms, including the multicellular ones, contain a single member. When a phylogenetic tree was constructed based on multiple alignment of the sequences listed in Table S1 in the supplemental material, several clusters that resembled the phylogenetic groups were generated (see Fig. S1B in the supplemental material). Thus, the *Ascomycetae*, *Euscomycetae*, and *Basidiomycetae* sequences became grouped separately from each other. Among the *Saccharomyces sensu stricto* species, two subgroups were generated, represented by *S. cerevisiae* Grx6 and Grx7, respectively. Most fungal sequences contain the N-terminal extension with the putative TM domain (see Table S1 and Fig. S1B in the supplemental material). On the contrary, the worm and plant homologues are shorter and lack this domain. In summary, monothiol Grxs with a putative TM domain seem characteristic for fungi, although TM-less relatives exist in other organisms.

**Grx6 and Grx7 localize at membranes of secretory vesicles.** Initially, we intended to obtain Grx6 and Grx7 derivatives tagged with GFP at the C termini in order to determine the cellular locations of both proteins in vivo. While the corresponding GFP constructions were obtained for Grx7, this was not possible for Grx6, even with other GFP-derived fluorescent tags. As an alternative, we marked Grx6 and Grx7 with the HA tag at the respective C termini by use of integrative plasmids. Several forms with slightly different gel mobilities were observed in the case of Grx6, and this was also the case for Grx7, although less prominently (Fig. 1; also see below). The respective Grx-HA strains were employed for sucrose gradient centrifugation analyses in the presence of Mg<sup>2+</sup> or EDTA to differentiate between ER and Golgi membranes (Fig. 1, left). Grx6 distributed in fractions that overlapped with the distribution of ER (Dpm1) and Golgi (Emp47) markers in EDTA-containing gradients. In Mg<sup>2+</sup> gradients, part of the Grx6 protein shifted to denser fractions corresponding to

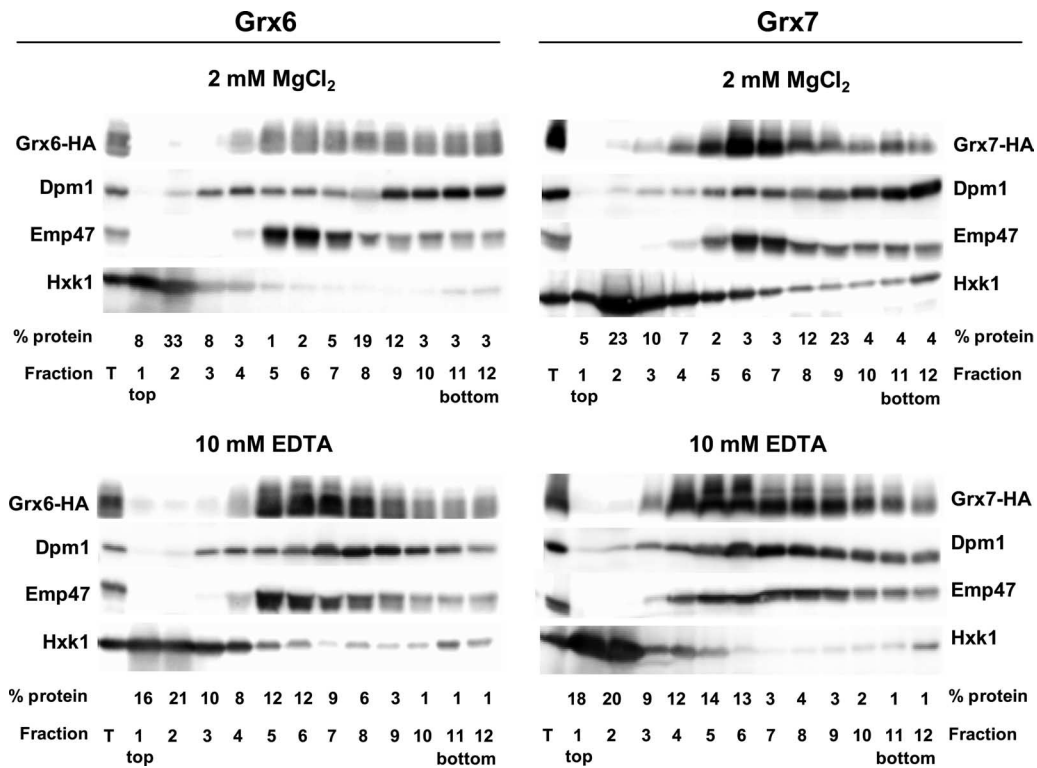


FIG. 1. Analysis of the association of Grx6 and Grx7 to membrane fractions. Exponentially growing cells (about  $3 \times 10^9$ ) in YEPD medium carrying a chromosomally integrated *GRX6-3HA* (MML897, left) or *GRX7-3HA* (MML999, right) fusion were employed for obtention of total cell extracts, which were clarified by low-speed centrifugation. The supernatant (fraction T) was subjected to 20% to 60% sucrose gradient centrifugation (5.5-ml total volume of the gradient) in the presence of 2 mM MgCl<sub>2</sub> or 10 mM EDTA. Each of the 12 resulting fractions was subjected to Western blot analysis to determine the distribution of Grx6-HA or Grx7-HA, Dpm1 (ER marker), Emp47 (Golgi marker), or Hxk1 (cytosolic marker), by use of adequate antibodies. Ten microliters from each fraction was analyzed in each lane, except for the lane for fraction T, which corresponds to 25  $\mu$ g of total protein. The relative distribution of total protein along the fractions is also indicated.

ribosome-associated microsomes, together with Dpm1, while another part remained in fractions cosedimenting with Emp47. In contrast, Grx7 sedimented in fractions containing the Golgi marker Emp47 in both Mg<sup>2+</sup> and EDTA gradients (Fig. 1, right).

The above observations are consistent with a distribution of Grx6 between ER and Golgi vesicles, while Grx7 would be mostly if not entirely located at the site of the Golgi apparatus. This confirms the study of Mesecke et al. (40), which also involved membrane subfractionation to demonstrate that Grx7 is located at Golgi vesicles. However, the present study extends these observations to indicate that in addition to fractionation to the Golgi, Grx6 also fractionates at ER membranes. To support the subfractionation analysis results, we carried out immunofluorescence studies with the Grx6-HA and Grx7-HA strains by use of anti-HA antibodies. Grx6 showed a perinuclear fluorescence pattern as well as a dotted distribution, while Grx7 mostly displayed a dotted distribution (Fig. 2A). With Ole1-GFP and Emp47 being used as markers for ER and Golgi compartments, respectively, the Grx6 perinuclear pattern overlapped with that of Ole1, while the Grx6 dotted distribution overlapped with Emp47 fluorescence (Fig. 2B). This dotted pattern is characteristic of Golgi proteins (59). It is important to remark that the analyses were done with cells that expressed *GRX6* under its own promoter. When cells were overloaded with Grx6 protein expressed from a multicopy plas-

mid, the perinuclear staining was predominant (not shown). Thus, immunofluorescence confirmed a distribution of Grx6 between the ER and Golgi compartments in physiological conditions. The dotted fluorescence of Grx7 also overlapped with Emp47 (Fig. 2B), confirming the predominant location of this protein in the Golgi apparatus. These patterns were not observed when Grx6 and Grx7 derivatives that lacked the TM domain deletions were analyzed ( $\Delta$ 3-40 and  $\Delta$ 3-36, respectively). These were localized in the entire cytoplasm (Fig. 2C). This observation emphasizes the importance of the domain for the membrane vesicle-associated distribution of Grx6 and Grx7.

In order to determine the membrane topology of Grx6 and Grx7, we obtained high-speed centrifugation microsomal fractions from cells expressing the respective HA derivatives, and these fractions were subjected to salt, carbonate (pH 11.5), urea, or Triton/salt treatments on ice. Only the last treatment was able to extract Grx7 partially (Fig. 3A), which indicates that Grx7 is most likely an integral membrane protein, as shown in a previous study (40). Grx6 was not extracted at all under these conditions, even in the presence of the detergent. We had to employ stronger extraction conditions (presence of the detergent during cell lysis) to partially release Grx6 from the membranous vesicle fraction (Fig. 3B). Therefore, Grx6

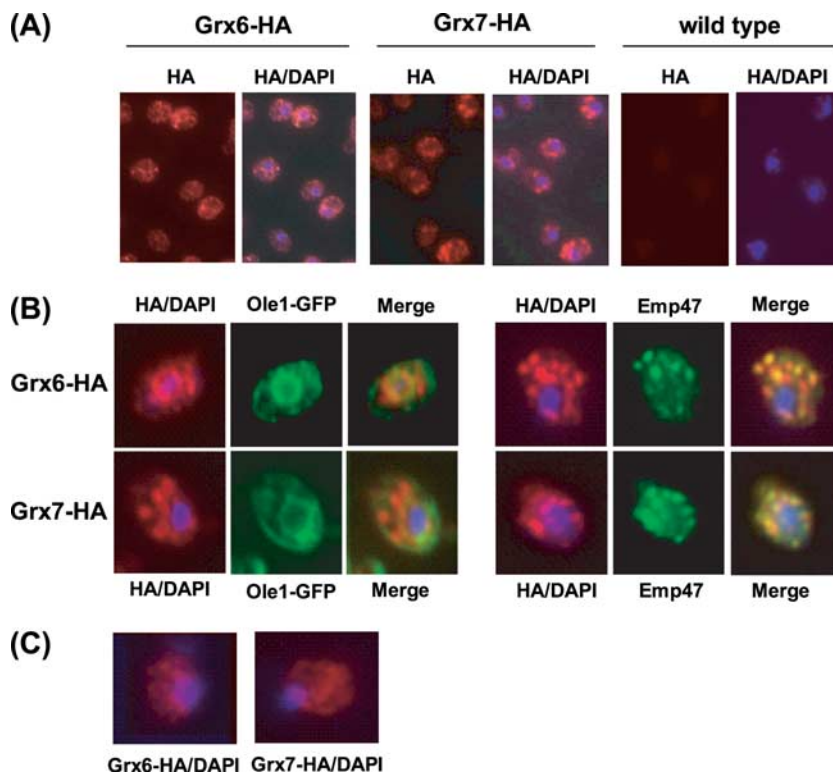


FIG. 2. Immunolocalization of Grx6 and Grx7. (A) Exponentially growing cells in YEPD medium and carrying a chromosomally integrated *GRX6-3HA* (MML897) or *GRX7-3HA* (MML999) fusion were analyzed by immunofluorescence with anti-HA antibodies. Nuclei were detected by DAPI (4',6'-diamidino-2-phenylindole) staining. (Right) Wild-type (W303-1A) cells treated with anti-HA antibodies. (B) Strains MML897 and MML999 were analyzed by immunofluorescence for colocalization of Grx6 or Grx7 and the Golgi marker Emp47 by use of anti-HA and anti-Emp47 antibodies (right). Similarly, derivatives of the above-mentioned strains that also carried a chromosomal Ole1-GFP fusion as an ER marker (MML1001 for the *GRX6-HA* strain and MML1003 for the *GRX7-HA* strain) were analyzed for colocalization, using anti-HA antibodies and GFP fluorescence analysis (left). Nuclei were detected by DAPI staining. (C) Cells expressing partially deleted versions of HA-tagged Grx6 ( $\Delta 3-40$ ; strain MML1037) or Grx7 ( $\Delta 3-36$ ; strain MML10399) were analyzed for immunolocalization with anti-HA antibodies. DAPI staining is also shown.

seems to be more strongly anchored at membranes than is Grx7.

Having shown that Grx6 and Grx7 are integral membrane proteins, we carried out proteinase K protection assays using Sec62-FLAG (integral ER membrane protein facing the cytosol) and Kar2-FLAG (luminal ER protein) as controls. Grx6 and Grx7 exhibited digestion patterns identical to that seen for Kar2 and contrary to that for Sec62; that is, they were protected from proteinase K digestion unless the membranes were permeabilized with Triton (Fig. 3C). We conclude that both Grx6 and Grx7 are integral membrane proteins with the glutaredoxin domain facing the vesicle lumen.

***GRX6* and *GRX7* expression is induced under diverse stress conditions.** Analysis of the respective promoter sequences revealed a calcineurin-dependent response element in the *GRX6* promoter, while the *GRX7* promoter contains a stress response element (STRE) (Fig. 4A). In *S. cerevisiae*, the calcineurin-dependent response element sequence is recognized by the Crz1 transcription factor, whose nucleocytoplasmic location and consequent transcriptional activity are under the control of the calcineurin phosphatase pathway (15, 41). This pathway is activated under specific stress conditions, such as exposition to high levels of  $\text{Ca}^{2+}$  or  $\text{Na}^+$ , heat shock, or incubation with  $\alpha$ -factor (70). The STRE is recognized by the Msn2/Msn4

transcription factor, which mediates a general environmental stress response in yeast cells upon exposition to heat, oxidative, and osmotic shocks among others (18). The presence of the respective response elements in the *GRX6* and *GRX7* promoters suggested that these two genes could respond to a number of external stresses. To test this hypothesis, we analyzed the expression levels of *GRX6* and *GRX7* under several stress conditions. Neither of the two genes responded to heat (25 to 37°C) or osmotic (1 M sorbitol) stress or to nutrient deprivation under postdiauxic growth conditions (data not shown). In contrast, *GRX6* expression was modestly upregulated by calcium, sodium, and oxidative stresses (Fig. 4B). In a Crz1-deficient mutant, such upregulation was partially eliminated, especially during sodium stress. The absence of Msn2/4 also negatively affected the induction of *GRX6* expression by those three stresses, probably indirectly, since the *GRX6* promoter does not contain STREs. Sodium and oxidative stresses, but not calcium stress, caused modest upregulation of *GRX7* expression. In this case, it was dependent on Msn2/Msn4 but not on Crz1 (Fig. 4B). We conclude that the Crz1-calcineurin pathway (for *GRX6*) and the Msn2/Msn4 factors (for *GRX7*) directly regulate the activation of these *GRX* genes after exposition to a specific set of stress conditions.

Next, we determined how the above-mentioned stresses in-

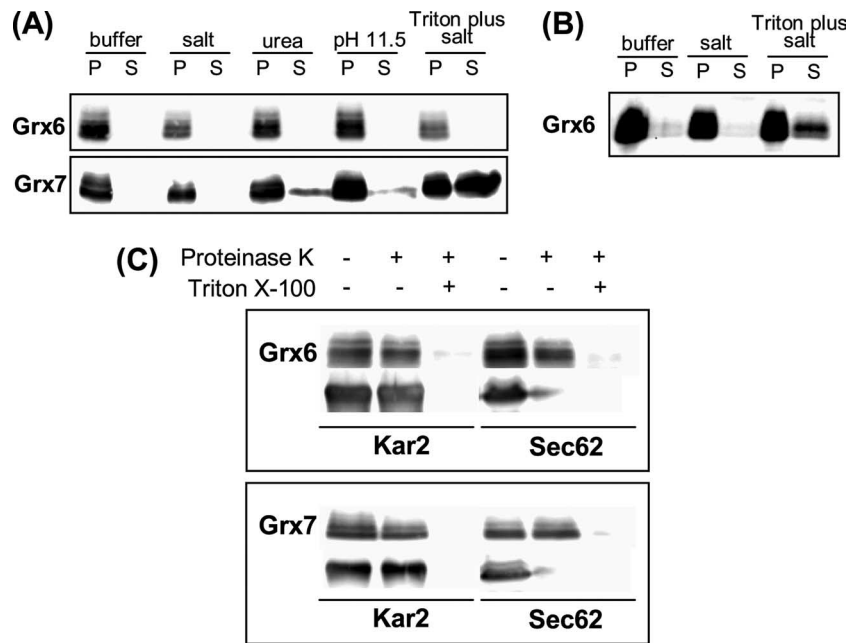


FIG. 3. Membrane topology of Grx6 and Grx7. (A) Extracts from exponentially growing cultures in YEPD ( $1.5 \times 10^9$  cells) of MML897 (*GRX6-3HA*) and MML999 (*GRX7-3HA*) strains were divided into five aliquots, which were treated (at  $0^\circ\text{C}$ ) with buffer or buffer plus 0.5 M NaCl, 2.5 M urea, 0.1 M  $\text{Na}_2\text{CO}_3$  (pH 11.5), or 1% Triton X-100 plus 0.5 M NaCl followed by high-speed centrifugation for separation into pellet (P) and supernatant (S) fractions. These were analyzed by Western blotting with anti-HA antibodies. Each line corresponds to the protein equivalent of  $5 \times 10^7$  cells. (B) Western blot of extracts from MML897 cells which were obtained after breaking the cells as described for panel A, except that 0.5 M NaCl or 1% Triton X-100 plus 0.5 M NaCl was present in the lysis buffer. Cell lysis was immediately followed by high-speed centrifugation to separate into pellet and supernatant fractions. (C) Extracts from exponentially growing cultures in YEPD ( $1.5 \times 10^9$  cells) of MML1013 (*GRX6-3HA KAR2-6FLAG*), MML1014 (*GRX6-3HA SEC62-6FLAG*), MML1011 (*GRX7-3HA KAR2-6FLAG*), and MML1012 (*GRX7-3HA SEC62-6FLAG*) strains were divided into three aliquots, which were mock treated or treated with proteinase K in the presence or absence of Triton X-100. Proteins were precipitated and analyzed by Western blotting with anti-HA antibodies.

fluence the levels of the Grx6 and Grx7 proteins. Calcium and sodium stresses did not significantly affect the amount of Grx6 (Fig. 5A). However, there was a temporary enrichment in the relative amount of the lower-mobility Grx6 forms, to return to the original situation at late times. Upon exposition to *tert*-butyl hydroperoxide (*t*-BOOH), there was a temporary increase of total Grx6 protein and a sustained accumulation of the low-mobility bands. Although 1 M sorbitol did not upregulate *GRX6* expression (Fig. 4B) and did not increase protein levels (Fig. 5A), after 20 min of osmotic stress almost all the Grx6 protein had been converted into lower-mobility species, to recover to basal conditions after 80 min. We also tested the effect of calcium or sodium stresses on Grx7 (Fig. 5A). In accordance with the kinetics of *GRX7* expression, Grx7 levels did not increase upon exposition to a high level of calcium (in fact, the protein amounts decreased at late time points), while sodium stress caused a large accumulation of Grx7. It should be noted that the Western blot of sodium-treated Grx7-HA cells shown in Fig. 5A was less exposed than were those in other cases; therefore, basal levels cannot be compared with those in other experiments. In those cases when Western blots were overexposed, such as for calcium-treated Grx7-HA cells, some lower-mobility Grx7 bands could also be observed (Fig. 5A). No changes in the cellular locations of Grx6 and Grx7 under calcium, sodium, oxidative, and osmotic stresses were appreciated during immunolocalization experiments (data not shown).

In order to determine whether the heterogeneity of Grx6 and Grx7 depends on their membrane-associated location, we subjected yeast cells carrying the HA-tagged wild-type proteins or the derivatives lacking the respective TM domains to sorbitol stress. Both TM-deleted Grx6 and Grx7 forms extracted from untreated cells migrated as sharp single bands in gels, and no lower-mobility bands appeared due to stress (Fig. 5B). Therefore, the extensive modification of Grx6 and, to a lesser extent, also of Grx7 occurs only in the membrane-associated forms.

We focused our attention on Grx6 to determine the type of modification affecting protein mobility in gels. Neither shrimp alkaline phosphatase treatments affected the migration of immunoprecipitated Grx6-HA protein (not shown), strongly indicating that phosphorylation was not involved. We then tested whether interfering with the ER/Golgi partition of Grx6 affected the extent of sorbitol-induced protein modification by using a temperature-sensitive *sec18* strain that accumulates ER membrane vesicles at  $37^\circ\text{C}$ . In fact, at the restrictive temperature Grx6 was modified only to a minor extent (Fig. 5C), while full modification occurred in the wild-type strain at  $37^\circ\text{C}$  (not shown). These observations indicated that extensive modification of Grx6 upon sorbitol treatment required movement into Golgi membranes. Many yeast proteins associated with the secretory machinery are subjected to N- or O-linked glycosylation. The ER and Golgi location of Grx6 suggested that the protein modification could be glycosylation. The fact

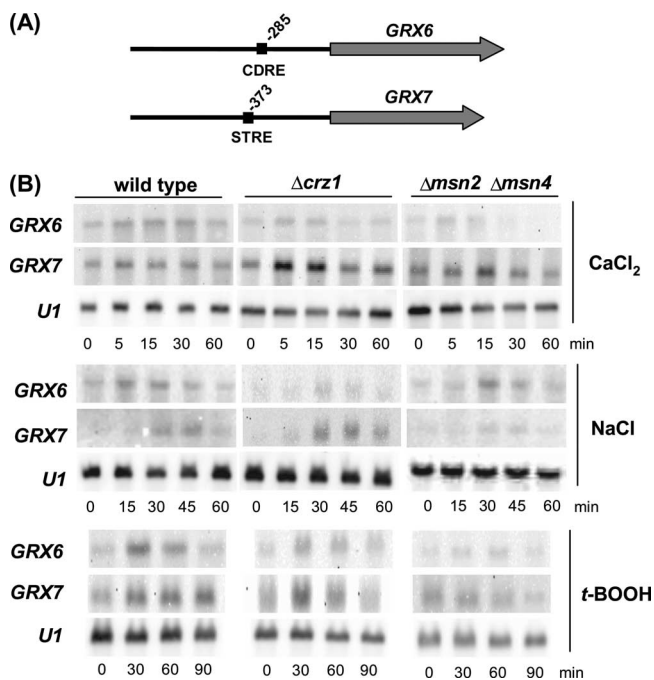


FIG. 4. Northern blot analysis of the expression of *GRX6* and *GRX7*. (A) Structure of the *GRX6* and *GRX7* promoters. CDRE, calcineurin-dependent response element. (B) Expression of *GRX6* and *GRX7* after the addition of 0.2 M CaCl<sub>2</sub>, 0.6 M NaCl, or 1 mM *t*-BOOH. Cells from wild-type (W303-1A) and the respective isogenic  $\Delta crz1$  (MML871) and  $\Delta msn2 \Delta msn4$  (Wmsn2msn4) strains were grown exponentially in YEPD medium. When cultures reached a concentration of  $1.5 \times 10^7$  cells per ml, the agent was added at the indicated concentration (time zero), and samples were obtained at the indicated times for expression analysis. A total of 25  $\mu$ g of total RNA was run per lane. U1 RNA was used to confirm that all lanes were equally loaded.

that tunicamycin (an inhibitor of N-linked glycosylation) still induced changes in Grx6 gel mobility (see below) ruled out this type of glycosylation as a source of Grx6 heterogeneity. On the other hand, in yeast cells O-linked glycosylation of Ser or Thr residues begins at the ER by the addition of a single mannose unit and continues at the Golgi by the addition of up to four additional mannose units (61). A family of ER *O*-mannosyltransferases coded by the *PMT1* to *-6* genes is involved in the addition of the first mannose residue, with partial substrate specificity (22). We therefore tested sorbitol-induced modification in different  $\Delta pmt$  mutants that expressed the Grx6-HA protein. In the genetic background employed (BY4741), Grx6 displayed a higher degree of modification than in other backgrounds in basal untreated conditions (Fig. 5D). In any case, a  $\Delta pmt2$  mutant had mostly inhibited the modification of Grx6 both before and after sorbitol treatment (Fig. 5D). The modification of Grx6 was also partially inhibited in a  $\Delta pmt1$  mutant, although to a lesser extent. The above results suggest that the modification of Grx6 consists of the addition of O-linked saccharides at the ER and Golgi compartments.

**ER stress causes accumulation of Grx6 and Grx7 proteins.** ER stress is provoked by situations leading to the accumulation of unfolded proteins at the lumen of this organelle, for instance after treatment with the reducing agent dithiothreitol or the

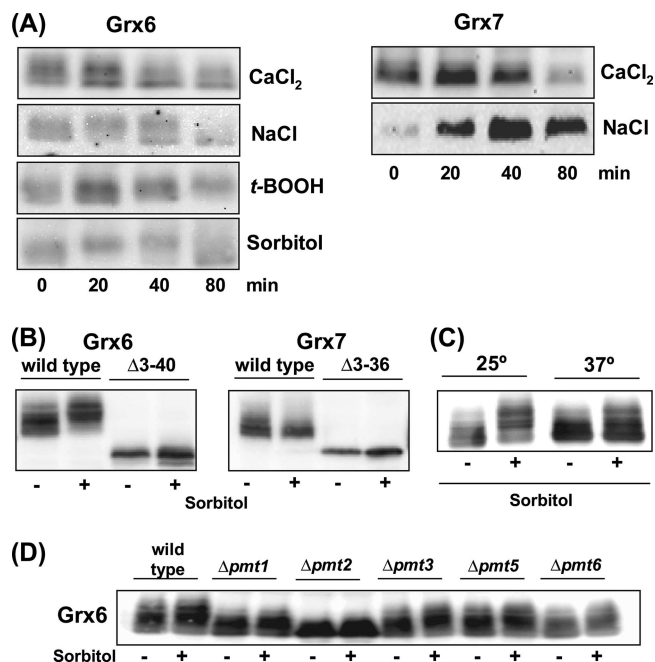


FIG. 5. Effect of several stresses on Grx6 and Grx7 proteins. (A) Cells of the MML953 (*GRX6-3HA::hphNT1*) and MML949 (*GRX7-3HA::hphNT1*) strains growing exponentially in YEPD medium were treated at the indicated times with 0.2 M CaCl<sub>2</sub>, 0.6 M NaCl, 1 mM *t*-BOOH, or 1 M sorbitol. Total cell extracts (20  $\mu$ g protein per lane) were subjected to Western blot analysis with anti-HA antibodies. (B) The following strains growing exponentially in YEPD medium were subjected to 1 M sorbitol treatment for 30 min and analyzed by Western blotting (20  $\mu$ g total cell protein per lane) with anti-HA antibodies: MML897 (expressing wild-type Grx6-HA), MML1037 ( $\Delta 3-40$  Grx6 deletion), MML999 (wild-type Grx7-HA), and MML1039 ( $\Delta 3-36$  Grx7 deletion). (C) MML1010 cells (*sec18ts GRX6-3HA*) were grown exponentially at 25°C in YEPD and treated with 1 M sorbitol for 30 min. A fraction of the culture was shifted to 37°C and, after 2 h, was also subjected to sorbitol treatment. Samples were taken for Western blot analysis (20  $\mu$ g total cell protein per lane) with anti-HA antibodies. (D) Wild-type BY4741 cells or *pmt* mutant derivatives (Y03792 [ $\Delta pmt1$ ], Y00385 [ $\Delta pmt2$ ], Y01618 [ $\Delta pmt3$ ], Y03790 [ $\Delta pmt5$ ], Y04829 [ $\Delta pmt6$ ]) transformed with pMM892 (centromeric plasmid expressing *GRX6-3HA* under its own promoter) were grown exponentially in SC medium and subjected to 1 M sorbitol treatment for 30 min. Samples were analyzed by Western blotting (20  $\mu$ g total cell protein per lane) with anti-HA antibodies.

N-linked glycosylation inhibitor tunicamycin. In these conditions, the unfolded protein response (UPR) is induced to up-regulate secretory pathway functions and to enhance protein refolding (49, 58). Thus, genes involved in disulfide bond formation, in chaperone activity, and in N- and O-linked glycosylation participate in the UPR in *S. cerevisiae* (62). However, tunicamycin also induces an UPR-independent response mediated by calcineurin (5). We determined whether ER stress due to tunicamycin affected the expression of *GRX6* and *GRX7*. Northern analyses demonstrated that both genes were upregulated upon ER stress (Fig. 6A). The induction of *GRX6* was partially dependent on Crz1, and a minor (probably indirect) dependence on Msn2/Msn4 was also observed. In contrast, the induction of *GRX7* expression was significantly reduced in the absence of Msn2/Msn4, while it did not depend on Crz1 (Fig. 6A). In parallel, tunicamycin treatment caused a

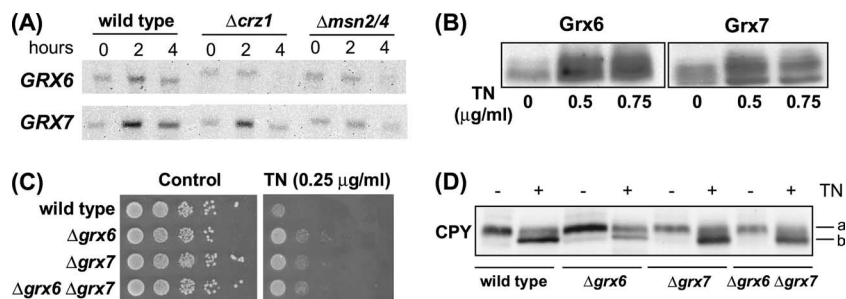


FIG. 6. Relationship between tunicamycin (TN)-induced ER stress and Grx6/Grx7. (A) Northern analysis of *GRX6* and *GRX7* expression after the addition of TN (0.75  $\mu\text{g/ml}$ , time zero) to cells from wild-type (W303-1A) and the respective isogenic  $\Delta\text{crz1}$  (MML871) and  $\Delta\text{msn2} \Delta\text{msn4}$  (Wmsn2msn4) strains growing exponentially in YEPD medium. Samples were obtained at the indicated times for expression analysis. A total of 25  $\mu\text{g}$  of total RNA was run per lane. (B) Western blot analysis of Grx6-HA and Grx7-HA levels in cells from strains MML953 (*GRX6-3HA::hphNTI*) and MML949 (*GRX7-3HA::hphNTI*) expressing the respective tagged chromosomal genes. Exponential cells in YEPD medium were treated for 4 h with the indicated TN concentration before Western blot analysis of total cell extracts (20  $\mu\text{g}$  per lane) with anti-HA antibody. (C) Sensitivity of W303-1A, MML890, MML887, and MML892 cells to TN in YEPD plates after 3 days of incubation (1:10 serial dilutions of exponential cultures) at 30°C. (D) Western blot of CPY for exponentially growing W303-1A, MML890, MML887, and MML892 cells untreated or treated for 4 h with TN at 0.5  $\mu\text{g/ml}$ . The mobilities of N-glycosylated (band a) and non-N-glycosylated (band b) forms are indicated.

dramatic increase in the amount of Grx6 and Grx7 proteins, especially of the more extensively O-glycosylated forms (Fig. 6B). All these observations established a relationship between Grx6/Grx7 and ER stress.

**Mutants deficient in Grx6 and Grx7 show moderate resistance to tunicamycin.** We tested the sensitivities of the single  $\Delta\text{grx6}$  and  $\Delta\text{grx7}$  mutants and the double mutant to some of the agents that upregulated expression of *GRX6* and *GRX7*. However, none of the mutants displayed differential sensitivity (relative to wild-type cells) to  $\text{CaCl}_2$ , NaCl, or *t*-BOOH (data not shown). Also, the mutants did not exhibit significant differences with respect to sensitivity to diamide, high temperature (37°C), alkaline conditions (pH 8), cadmium, osmotic stress by KCl, or dithiothreitol. In a previous study (40), a mutant lacking Grx6 was hypersensitive to hydrogen peroxide, while the absence of any amount of either Grx caused growth defects at 37°C. These discrepancies can be caused by the different genetic backgrounds employed in both studies. However, under our conditions the single and double mutants displayed a moderate resistance to tunicamycin (Fig. 6C). This effect was not due to the drug being unable to act at the ER environment of the mutants, since it was still able to inhibit the N glycosylation of CPY in the single and double mutants (Fig. 6D). Since the induction of the protein kinase C pathway in *S. cerevisiae* and the consequent activation of the Slt2 mitogen-activated kinase leads to tunicamycin resistance (9), we analyzed whether Slt2 was constitutively activated in the mutants. However, this was not the case (data not shown). Nevertheless, these results confirm a functional relationship between ER stress and Grx6/Grx7 (see Discussion).

**Grx6 and Grx7 display thiol oxidoreductase activity in vivo.** Grx6 and Grx7 have been shown to possess thiol oxidoreductase activity in vitro (39, 40). To demonstrate that both proteins also display such activity under physiological conditions, we constructed two strains that overexpressed Grx6 and Grx7, respectively, in a genetic background that lacked the standard dithiol glutaredoxins Grx1 and Grx2. Extracts from such yeast cells had thiol oxidoreductase activity significantly higher than that seen for control cells, and this activity increased between 1.5- and 2-fold after tunicamycin treatment (Fig. 7A). On the

contrary, the overexpression of mutant forms of *GRX6* or *GRX7* in which the active-site cysteine residues had been changed to serine did not increase the thiol oxidoreductase activity over background levels (data not shown). These results confirmed that the enzyme activity of Grx6 and Grx7 is present in vivo and that it parallels the increase of protein levels during the ER stress due to tunicamycin. Significantly, extracts overexpressing Grx7 had higher activity than those overexpressing Grx6 (Fig. 7A), in accordance with results from reference 40, indicating that purified Grx7 is more active in HEDS assays than is Grx6. Next, we determined whether conditions (1 M sorbitol treatment) that induce over-O-glycosylation of Grx6 cause changes in the in vivo activity of the protein without affecting total protein levels. However, thiol oxidoreductase activity levels remained approximately constant during the osmotic stress by sorbitol (Fig. 7B), demonstrating that the activity is not affected by the modification of the protein in these conditions.

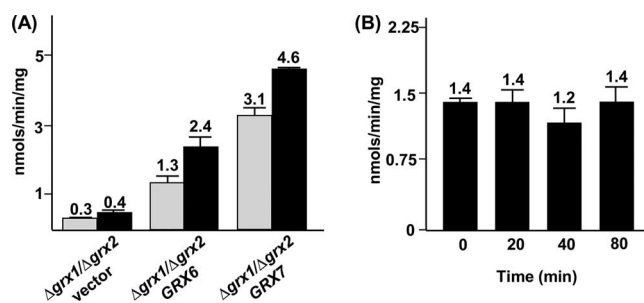


FIG. 7. In vivo thiol oxidoreductase activity of Grx6 and Grx7. (A) Enzyme activity (expressed as nmol/min/mg total cell protein) in MML752 ( $\Delta\text{grx1} \Delta\text{grx2}$ ) cells transformed with the YEplac195 vector or the multicopy plasmid derivatives pMM822 (*GRX6* expression) and pMM763 (*GRX7* expression) and growing exponentially in SC medium. Gray and black bars correspond to untreated and tunicamycin (0.5  $\mu\text{g/ml}$ , 2 h)-treated cultures, respectively. Values over bars are the means from three experiments. (B) Enzyme activity in pMM822-transformed MML752 cells growing exponentially in SC medium and treated with 1 M sorbitol for the indicated times. Values are the means from three experiments.

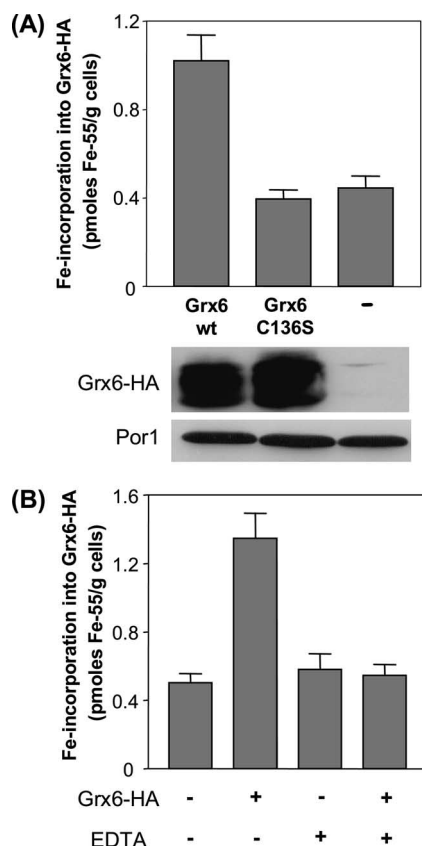


FIG. 8. Grx6 binds iron in vivo. (A) Wild-type cells and cells overexpressing wild-type (wt) Grx6-HA and the C136S mutant from plasmids pMM866 and pMM880, respectively, were grown overnight in iron-free SC medium containing glucose. Cells were labeled with 10  $\mu\text{Ci}$   $^{55}\text{Fe}$  for 2 h. Cells were harvested, washed, and transferred to an anaerobic chamber. Cells were resuspended in anaerobic Tris-buffered saline-Tween buffer, and crude cell extracts were prepared by lysis with glass beads. Grx6 was immunoprecipitated from extracts with anti-HA antiserum under anaerobic conditions and the level of coimmunoprecipitated radioactivity was quantified by scintillation counting. The total amount of Grx6 in the extracts was assessed by immunostaining. Por1p was used as a loading control. (B) Wild-type cells and cells overexpressing wild-type Grx6-HA were radiolabeled with  $^{55}\text{Fe}$ , and Grx6 was immunoprecipitated with anti-HA antibodies as described above. Following the sedimentation of the immunobeads, the beads were washed three times with buffer either lacking EDTA (-) or supplemented with 2.5 mM EDTA (+) under anaerobic conditions. Error bars indicate the standard deviations of the measurements.

**Grx6 binds iron in vivo.** Monothiol Grxs including Grx6 harbor a Fe/S cluster cofactor upon recombinant expression in *Escherichia coli* (39). We have confirmed that observation and also that recombinant Grx7 does not contain such a cluster. In order to analyze whether Grx6 binds iron in *S. cerevisiae* in vivo, a HA-tagged version of Grx6 was overexpressed in wild-type cells from the high-copy-number vector pMM866 under the control of its own promoter. Cells were grown in iron-poor SD medium (60) for 16 h and radiolabeled with  $^{55}\text{Fe}$  for 2 hours. Whole-cell lysates were prepared under anaerobic conditions, and Grx6 was immunoprecipitated with anti-HA antibodies. The amount of  $^{55}\text{Fe}$  bound to the immunobeads reflects the amount of iron bound to Grx6 and was quantified by scintillation counting (Fig. 8A). A rather small but significant

amount of radioactive  $^{55}\text{Fe}$  ( $\sim 1$  pmol  $^{55}\text{Fe}/\text{g}$  cells) coprecipitated with anti-HA antibodies from cells overproducing Grx6-HA. Only background levels of radioactivity ( $< 0.4$  pmol  $^{55}\text{Fe}/\text{g}$  cells) were detected when we used cells that did not contain Grx6-HA or that overproduced the site-directed mutant that carried a C136S mutation in the conserved active-site cysteine of Grx6. Iron association to Grx6-HA declined to background levels upon incubation of the immunoprecipitated protein with EDTA (Fig. 8B). Taken together, these results demonstrate that Grx6 binds iron with low affinity in a labile fashion at its active-site cysteine when overproduced in yeast cells. However, the low affinity of Grx6 for iron precluded any attempts to determine whether the iron is bound in form of a Fe/S cluster on Grx6 in vivo.

## DISCUSSION

Eukaryotic Grxs are present in such different compartments as the cytosol, nucleus, mitochondria, and chloroplasts, carrying out a diverse array of functions as regulators of thiol redox state (19, 28). Here we describe two *S. cerevisiae* monothiol Grxs located at the ER and/or Golgi membranes and facing the luminal side of the vesicles. Homologues of these two Grxs with similar structures exist in different fungal groups. A *Schizosaccharomyces pombe* homologue of Grx6/Grx7 which also manifests the perinuclear distribution of ER proteins has been described previously (12).

Is the lumen of secretory vesicles adequate for the enzyme activity of Grx6 and Grx7? The ER lumen is an oxidizing environment which favors the activity of protein disulfide isomerase (PDI) in the formation of native disulfide bonds in proteins of the secretory pathway. Among the large number of species of the PDI family in human cells, four of them are ER membrane associated, facing the vesicle lumen (17). In the ER lumen, reactive oxygen species are generated mostly as a side effect of the action of Ero1 thiol oxidase on its substrate, PDI (26). This is in accordance with the observation that the ratio between GSH and oxidized glutathione is much lower in the lumen of secretory vesicles than in the cytosol (30) and that a majority of glutathione molecules in ER microsomes exist as mixed disulfides with resident proteins (1). While protein glutathionylation can be contemplated as a mechanism for temporary protection against the irreversible oxidation of cysteine residues, the restoration of native sulfhydryl groups is a prerequisite for protein functionality. PDI is able to carry out the deglutathionylation reaction concomitantly with the formation of native disulfide bonds (8). Grx6 or Grx7 could also be able to catalyze this reaction and thus to regulate the redox state of protein sulfhydryl groups in the lumen of the ER/Golgi. In fact, the monothiol mechanism of action of Grxs involves resolving mixed disulfides between GSH and protein sulfhydryls in a process that requires a single reduced cysteine in the Grx molecule and results in a mixed disulfide between GSH and Grx (6). GSH is subsequently required for the reduction of the mixed disulfide and the regeneration of the active enzyme. The question remains whether GSH could act as such a Grx reductant in the oxidizing environment of the ER. GSH could be generated by the action of PDI at the ER lumen (8). Also, in yeast cells, the depletion of GSH rescues the phenotypic defects of an *ero1* mutant caused by excessive PDI reduction,

which led to the interpretation that GSH can act as a net reductant in the ER (14). Notably, *E. coli* Grx1 is able to act as a disulfide oxidase in *in vitro* assays, using the monothiol mechanism more efficiently than PDI (69). In *in vitro* assays, Grx7 has no protein-refolding activity (40). This requires disulfide reduction in addition to sulfhydryl oxidation and is characteristic of PDI enzymes. Nevertheless, there is a possibility that Grx6 and Grx7 carry out the deglutathionylation of GSH-mixed disulfides concomitantly with disulfide bond formation in the oxidant environment of the early secretory pathway.

Although Grx6 and Grx7 are structurally similar, there are a number of differences that point to at least partially different cellular functions. First, recombinant Grx6 is a Fe/S protein while Grx7 is not, which is an effect of the active-site differences that exist among them (3, 39, 57). Another difference concerns their cellular distributions, namely, ER and Golgi for Grx6 and Golgi for Grx7. This asymmetric distribution may explain their differences in O-glycosylation pattern, which is more extensive in Grx6, even in unstressed cells. Saccharide chain extension begins at the ER with a first mannose unit to continue at the Golgi (61), with ER-located complexes between Pmt1 and Pmt2 playing a main role in substrate recognition and the addition of the first mannose (24). Pmt2 and (to a minor extent) Pmt1 are responsible for initiating the O glycosylation of Grx6. We do not know whether there is an ER and Golgi recycling of Grx6 molecules or whether there are permanent subpopulations at both compartments, although in any case the ER Grx6 pool would become prone to O-mannose modification at some of the 24 serine or 11 threonine residues of the molecule and to eventual chain extension when reaching the Golgi membranes.

Grx6 and Grx7 also differ with respect to transcriptional regulation in response to a number of stresses and the transcription factors involved. The modest upregulation of *GRX6* expression in response to calcium, sodium, and oxidative stresses depends in part on the Crz1-calcineurin pathway. In response to calcium and sodium, this pathway regulates the expression of genes that participate in transport of small molecules, ion homeostasis, cell wall synthesis and remodeling, or vesicle transport (70), that is, in functions which in many cases can be related to secretory compartments. At the protein level, among those stresses only oxidative stress caused a transient increase in amount of Grx6. However, temporary accumulation of the most O-glycosylated forms occurred after the stress. There are no previous reports on the increment of activity of the Pmt proteins after such stress conditions. We can hypothesize that the transient increase of the extensively O-glycosylated forms may be due to transient protein accumulation in the ER, which we have not been able to detect microscopically. The response of *GRX7* expression to the indicated stresses is more modest than that of *GRX6* and seems to be part of the Msn2/4-mediated environmental stress response. However, among all the conditions tested, sodium ion stress resulted in the most intense Grx7 response. A different situation is the response of *GRX6* and *GRX7* to ER stress by tunicamycin. Both genes are upregulated under such a condition, in manners dependent on Crz1 and Msn2/4, respectively, and this is paralleled by protein accumulation. Tunicamycin provokes two kinds of responses in yeast cells: the Ire1- and Hac1-mediated UPR for protein refolding (62) and the Pkc1/Slt2 and cal-

calcineurin/Crz1-mediated response for cell survival (4, 5). *GRX6* and *GRX7* seem to respond only to the Crz1 pathway, as neither of these genes have been described as UPR targets in two independent studies (34, 62).

What could be the function of Grx6 and Grx7 at the secretory apparatus? They do not seem to play a general role in protein N glycosylation and/or folding, as (i) a reporter protein, CPY, is correctly N glycosylated in cells lacking one or both Grxs (this work); and (ii) the UPR is not constitutively induced in either the single or the double mutant (40). The mutants, however, behave similarly with respect to their increased resistance to tunicamycin. Previous observations related redox regulation, oxidative stress, and tunicamycin resistance in yeast cells. A mutant lacking cytosolic thioredoxin reductase (Trr1) is hyperresistant to tunicamycin, while a double mutant in the two cytosolic thioredoxins is not (63). This suggests a connection between tunicamycin stress and some targets of Trr1 other than thioredoxins. On the other hand, Eos1 is an ER membrane protein whose absence causes hypersensitivity to oxidative stress, tolerance to growth inhibition by tunicamycin, and resistance to the N-glycosylation-inhibitory effect of the drug (46). The Eos1 primary sequence, however, does not allow this protein to be associated with specific biochemical functions. In the case of the *grx6* and *grx7* mutants, the drug remains active as an N-glycosylation inhibitor of specific secretory proteins such as CPY. N-glycosylation defects or ER stress caused by tunicamycin (in combination with temperature increase to 37°C) induces apoptotic effects in yeast cells (27). ER stress also induces apoptosis in mammalian cells (11, 16). Grx6 and Grx7 could be regulating the redox state of cysteine residues required for the activity of specific proteins in the ER or Golgi compartments, some of which could be required as intermediates in the cascade inducing apoptosis. Since Grx6 and Grx7 are restricted to fungal membranes, such regulatory functions in the membranes of the secretory vesicles, if conserved, should be carried in higher eukaryotes by other thiol oxidoreductases, such as some of the PDI species.

#### ACKNOWLEDGMENTS

This work was supported by grants BFU2004-03167 and CSD2007-0020 (Ministerio de Educación y Ciencia) and 2005SGR-00677 (Generalitat de Catalunya) to E.H. and by grant SFB 593 (Deutsche Forschungsgemeinschaft) to U.M. A.I. is the recipient of a predoctoral grant from Ministerio de Educación y Ciencia, Spain.

We thank M. Aldea and P. Sanz for biological materials and helpful suggestions and Lidia Piedrafito for technical assistance.

#### REFERENCES

1. Bass, R., L. W. Ruddock, P. Klappa, and R. B. Freedman. 2004. A major fraction of endoplasmic reticulum-located glutathione is present as mixed disulfides with protein. *J. Biol. Chem.* **279**:5257–5262.
2. Bellí, G., E. Gari, L. Piedrafito, M. Aldea, and E. Herrero. 1998. An activator/repressor dual system allows tight tetracycline-regulated gene expression in budding yeast. *Nucleic Acids Res.* **26**:942–947.
3. Berndt, C., C. Hudemann, E. M. Hanschmann, R. Axelsson, A. Holmgren, and C. H. Lillig. 2007. How does iron-sulfur cluster coordination regulates the activity of human glutaredoxin 2? *Antioxid. Redox Signal.* **9**:151–157.
4. Bonilla, M., and K. W. Cunningham. 2003. Mitogen-activated protein kinase stimulation of Ca<sup>2+</sup> signaling is required for survival of endoplasmic reticulum stress in yeast. *Mol. Biol. Cell* **14**:4296–4305.
5. Bonilla, M., K. K. Nastase, and K. W. Cunningham. 2002. Essential role of calcineurin in response to endoplasmic reticulum stress. *EMBO J.* **21**:2343–2353.
6. Bushweller, J. H., F. Aslund, K. Wuthrich, and A. Holmgren. 1992. Structural and functional characterization of the mutant *Escherichia coli* glutare-

- doxin (C14-S) and its mixed disulfide with glutathione. *Biochemistry* **31**: 9288–9293.
7. Camaschella, C., A. Campanella, L. De Falco, L. Boschetto, R. Merlini, L. Silvestri, S. Levi, and A. Iolascon. 2007. The human counterpart of zebrafish shiraz shows sideroblastic-like microcytic anemia and iron overload. *Blood* **110**:1353–1358.
  8. Chakravarthi, S., C. E. Jessop, and N. J. Bulleid. 2006. The role of glutathione in disulphide bond formation and endoplasmic-reticulum-generated oxidative stress. *EMBO Rep.* **7**:271–275.
  9. Chen, Y., D. E. Feldman, C. Deng, J. A. Brown, A. F. De Giacomo, A. F. Gaw, G. Shi, Q. T. Le, J. M. Brown, and A. C. Koong. 2005. Identification of mitogen-activated protein kinase signaling pathways that confer resistance to endoplasmic reticulum stress in *Saccharomyces cerevisiae*. *Mol. Cancer Res.* **3**:669–677.
  10. Cheng, N. H., J. Z. Liu, A. Brock, R. S. Nelson, and K. D. Hirschi. 2006. AtGRXcp, an *Arabidopsis* chloroplast/plastidic glutaredoxin is critical for protection against protein oxidative damage. *J. Biol. Chem.* **281**:26280–26288.
  11. Chevet, E., P. H. Cameron, M. F. Pelletier, D. Y. Thomas, and J. J. Bergeron. 2001. The endoplasmic reticulum: integration of protein folding, quality control signaling and degradation. *Curr. Opin. Struct. Biol.* **11**:120–124.
  12. Chung, W. H., K. D. Kim, and J. H. Roe. 2005. Localization and function of three monothiol glutaredoxins in *Schizosaccharomyces pombe*. *Biochem. Biophys. Res. Commun.* **330**:604–610.
  13. Collinson, E. J., and C. M. Grant. 2003. Role of yeast glutaredoxins as glutathione S-transferases. *J. Biol. Chem.* **278**:22492–22497.
  14. Cuozzo, J. W., and C. A. Kaiser. 1999. Competition between glutathione and protein thiols for disulphide-bond formation. *Nat. Cell Biol.* **1**:130–135.
  15. Cyert, M. S. 2001. Genetic analysis of calmodulin and its targets in *Saccharomyces cerevisiae*. *Annu. Rev. Genet.* **35**:647–672.
  16. Delom, F., A. Emadali, E. Cocolakis, J. J. Lebrun, A. Nantel, and E. Chevet. 2007. Calnexin-dependent regulation of tunicamycin-induced apoptosis in breast carcinoma MCF-7 cells. *Cell Death Differ.* **14**:586–596.
  17. Elgaard, L., and L. W. Ruddock. 2005. The human protein disulphide isomerase family: substrate interactions and functional properties. *EMBO Rep.* **6**:28–32.
  18. Estruch, F. 2000. Stress-controlled transcription factors, stress-induced genes and stress tolerance in budding yeast. *FEMS Microbiol. Rev.* **24**:469–486.
  19. Fernandes, A. P., and A. Holmgren. 2004. Glutaredoxins: glutathione-dependent redox enzymes with functions far beyond a simple thioredoxin backup system. *Antioxid. Redox Signal.* **6**:63–74.
  20. Gallego, C., E. Gari, N. Colomina, E. Herrero, and M. Aldea. 1997. The Cln3 cyclin is down-regulated by translational repression and degradation during the G1 arrest caused by nitrogen deprivation in budding yeast. *EMBO J.* **16**:7196–7206.
  21. Garcera, A., L. Barreto, L. Piedrafita, J. Tamarit, and E. Herrero. 2006. *Saccharomyces cerevisiae* cells have three omega-class glutathione transferases acting as 1-Cys thiol transferases. *Biochem. J.* **398**:187–196.
  22. Gentsch, M., and W. Tanner. 1997. Protein-O-glycosylation in yeast: protein-specific mannosyltransferases. *Glycobiology* **7**:481–486.
  23. Gietz, R. D., and A. Sugino. 1988. New yeast-*Escherichia coli* shuttle vectors constructed with in vitro mutagenized yeast genes lacking six-base pair restriction sites. *Gene* **74**:3065–3073.
  24. Girrbach, V., and S. Strahl. 2003. Members of the evolutionarily conserved PMT family of protein O-mannosyltransferases form distinct protein complexes among themselves. *J. Biol. Chem.* **278**:12554–15562.
  25. Goldstein, A. L., and J. H. McCusker. 1999. Heterologous *URAMX* cassettes for gene replacement in *Saccharomyces cerevisiae*. *Yeast* **15**:507–511.
  26. Gross, E., C. S. Sevier, N. Heldman, E. Vit, M. Bentzur, C. A. Kaiser, C. Thorpe, and D. Fass. 2006. Generating disulfides enzymatically: reaction products and electron acceptors of the endoplasmic reticulum thiol oxidase Ero1p. *Proc. Natl. Acad. Sci. USA* **103**:299–304.
  27. Hauptmann, P., C. Riel, L. A. Kunz-Schughart, K. U. Fröhlich, F. Madeo, and L. Lehle. 2006. Defects in N-glycosylation induce apoptosis in yeast. *Mol. Microbiol.* **59**:765–778.
  28. Herrero, E., and M. A. de la Torre-Ruiz. 2007. Monothiol glutaredoxins: a common domain for multiple functions. *Cell. Mol. Life Sci.* **64**:1518–1530.
  29. Holmgren, A., and F. Aslund. 1995. Glutaredoxin. *Methods Enzymol.* **252**: 283–292.
  30. Hwang, C., A. J. Sinskey, and H. F. Lodish. 1992. Oxidized redox state of glutathione in the endoplasmic reticulum. *Science* **257**:1496–1502.
  31. Janke, C., M. M. Magiera, N. Rathfelder, C. Taxis, S. Reber, H. Maekawa, A. Moreno-Borchart, G. Doenges, E. Schwob, and M. Knop. 2004. A versatile toolbox for PCR-based tagging of yeast genes: new fluorescent proteins, more markers and promoter substitution cassettes. *Yeast* **21**:947–962.
  32. Johansson, C., K. L. Kavanagh, O. Gileadi, and U. Oppermann. 2007. Reversible sequestration of active site cysteines in a 2Fe-2S-bridged dimer provides a mechanism for glutaredoxin 2 regulation in human mitochondria. *J. Biol. Chem.* **282**:3077–3082.
  33. Juanes, M. A., J. C. Igual, and M. C. Bañó. 2008. Membrane topology and post-translational modification of the *Saccharomyces cerevisiae* essential protein Rot1. *Yeast* **25**:93–106.
  34. Kimata, Y., Y. Ishiwata-Kimata, S. Yamada, and K. Kohno. 2006. Yeast unfolded protein response pathway regulates expression of genes for anti-oxidative stress and for cell surface proteins. *Genes Cells* **11**:59–69.
  35. Lill, R., and U. Mühlenhoff. 2006. Iron-sulfur protein biogenesis in eukaryotes: components and mechanisms. *Annu. Rev. Cell Dev. Biol.* **22**:457–486.
  36. Lillig, C. H., C. Berndt, O. Vergnolle, M. E. Lonn, C. Hudemann, E. Bill, and A. Holmgren. 2005. Characterization of human glutaredoxin 2 as iron-sulfur protein: a possible role as redox sensor. *Proc. Natl. Acad. Sci. USA* **102**: 8168–8173.
  37. Lopreato, R., S. Facchin, G. Sartori, G. Arrigoni, S. Casonato, M. Ruzzene, L. A. Pinna, and G. Carignani. 2004. Analysis of the interaction between piD261/Bud32, an evolutionary conserved protein kinase of *Saccharomyces cerevisiae*, and the Grx4 glutaredoxin. *Biochem. J.* **377**:395–405.
  38. Luikenhuis, S., G. Perrone, I. W. Dawes, and C. M. Grant. 1998. The yeast *Saccharomyces cerevisiae* contains two glutaredoxin genes that are required for protection against reactive oxygen species. *Mol. Biol. Cell* **9**:1081–1091.
  39. Mesecke, N., S. Mittler, E. Eckers, J. M. Herrmann, and M. Deponte. 2008. Two novel monothiol glutaredoxins from *Saccharomyces cerevisiae* provide further insight into iron-sulfur cluster binding, oligomerization, and enzymatic activity of glutaredoxins. *Biochemistry* **47**:1452–1463.
  40. Mesecke, N., A. Spang, M. Deponte, and J. M. Herrmann. 2008. A novel group of glutaredoxins in the cis-Golgi critical for oxidative stress resistance. *Mol. Biol. Cell* **19**:2673–2680.
  41. Miyakawa, T., and M. Mizunuma. 2007. Physiological roles of calcineurin in *Saccharomyces cerevisiae* with special emphasis on its roles in G2/M cell cycle regulation. *Biosci. Biotechnol. Biochem.* **71**:633–645.
  42. Molik, S., R. Lill, and U. Mühlenhoff. 2007. Methods for studying iron metabolism in yeast mitochondria. *Methods Cell Biol.* **80**:261–280.
  43. Molina, M. M., G. Bellí, M. A. de la Torre, M. T. Rodríguez-Manzaneeque, and E. Herrero. 2004. Nuclear monothiol glutaredoxins of *Saccharomyces cerevisiae* can function as mitochondrial glutaredoxins. *J. Biol. Chem.* **279**: 51923–51930.
  44. Molina-Navarro, M. M., C. Casas, L. Piedrafita, G. Bellí, and E. Herrero. 2006. Prokaryotic and eukaryotic monothiol glutaredoxins are able to perform the functions of Grx5 in the biogenesis of Fe/S clusters in yeast mitochondria. *FEBS Lett.* **580**:2273–2280.
  45. Mühlenhoff, U., J. Gerber, N. Richhardt, and R. Lill. 2003. Components involved in assembly and dislocation of iron-sulfur clusters on the scaffold protein Isu1p. *EMBO J.* **22**:4815–4825.
  46. Nakamura, T., A. Ando, H. Takagi, and J. Shima. 2007. *EOS1*, whose deletion confers sensitivity to oxidative stress, is involved in N-glycosylation in *Saccharomyces cerevisiae*. *Biochem. Biophys. Res. Commun.* **353**:293–298.
  47. Nieto, A., R. Sentandreu, L. del Castillo-Agudo, and P. Sanz. 1993. Cloning and characterization of the *SEC18* gene from *Candida albicans*. *Yeast* **9**:875–887.
  48. Ojeda, L., G. Keller, U. Mühlenhoff, J. C. Rutherford, R. Lill, and D. R. Winge. 2006. Role of glutaredoxin-3 and glutaredoxin-4 in the iron-regulation of the Aft1 transcriptional activator in *Saccharomyces cerevisiae*. *J. Biol. Chem.* **281**:17661–17669.
  49. Patil, C., and P. Walter. 2001. Intracellular signaling from the endoplasmic reticulum to the nucleus: the unfolded protein response in yeast and animals. *Curr. Opin. Cell Biol.* **13**:349–356.
  50. Picciocchi, A., C. Saguez, A. Boussac, C. Cassier-Chauvat, and F. Chauvat. 2007. CGFS-type monothiol glutaredoxins from the cyanobacterium *Synechocystis* PCC6803 and other evolutionary distant model organisms possess a glutathione-ligated [2Fe-2S] cluster. *Biochemistry* **46**:15018–15026.
  51. Porras, P., C. A. Padilla, M. Krayl, W. Voos, and J. A. Bárcena. 2006. One single in-frame AUG codon is responsible for a diversity of subcellular localizations of glutaredoxin 2 in *Saccharomyces cerevisiae*. *J. Biol. Chem.* **281**:16551–16562.
  52. Pujol-Carrión, N., G. Bellí, E. Herrero, A. Nogués, and M. A. de la Torre-Ruiz. 2006. Glutaredoxins Grx3 and Grx4 regulate the nuclear localization of Aft1 and the oxidative stress response in *Saccharomyces cerevisiae*. *J. Cell Sci.* **119**:4554–4564.
  53. Roberg, K. J., N. Rowley, and C. A. Kaiser. 1997. Physiological regulation of membrane protein sorting late in the secretory pathway of *Saccharomyces cerevisiae*. *J. Cell Biol.* **137**:1469–1482.
  54. Rodríguez-Manzaneeque, M. T., J. Ros, E. Cabiscol, A. Sorribas, and E. Herrero. 1999. Grx5 glutaredoxin plays a central role in protection against protein oxidative damage in *Saccharomyces cerevisiae*. *Mol. Cell. Biol.* **19**: 8180–8190.
  55. Rodríguez-Manzaneeque, M. T., J. Tamarit, G. Bellí, J. Ros, and E. Herrero. 2002. Grx5 is a mitochondrial glutaredoxin required for the activity of iron/sulfur enzymes. *Mol. Biol. Cell* **13**:1109–1121.
  56. Rouhieh, N., J. Couturier, and J. P. Jacquot. 2006. Genome-wide analysis of plant glutaredoxin systems. *J. Exp. Bot.* **57**:1685–1696.
  57. Rouhieh, N., H. Unno, S. Bandyopadhyay, L. Masip, S. K. Kim, M. Hirasawa, J. M. Gualberto, V. Lattard, M. Kusunoki, D. B. Knaff, G. Georgiou, T. Hase, M. K. Johnson, and J. P. Jacquot. 2007. Functional, structural, and

- spectroscopic characterization of a glutathione-ligated [2Fe-2S] cluster in poplar glutaredoxin C1. *Proc. Natl. Acad. Sci. USA* **104**:7379–7384.
58. Schröder, M., and R. J. Kaufman. 2005. The mammalian unfolded protein response. *Annu. Rev. Biochem.* **74**:739–789.
59. Schröder, S., F. Schimmöller, B. Singer-Krüger, and H. Riezman. 1995. The Golgi-localization of yeast Emp47p depends on its di-lysine motif but is not affected by the *ret1-1* mutation in  $\alpha$ -COP. *J. Cell Biol.* **131**:895–912.
60. Sherman, F. 2002. Getting started with yeast. *Methods Enzymol.* **350**:3–41.
61. Strahl-Bolsinger, S., M. Gentsch, and W. Tanner. 1999. Protein O-mannosylation. *Biochim. Biophys. Acta* **1426**:297–307.
62. Travers, K. J., C. K. Patil, L. Wodika, D. J. Lockhart, J. S. Weissman, and P. Walter. 2000. Functional and genomic analyses reveal an essential coordination between the unfolded protein response and ER-associated degradation. *Cell* **101**:249–258.
63. Trotter, E. W., and C. M. Grant. 2002. Thioredoxins are required for protection against a reductive stress in the yeast *Saccharomyces cerevisiae*. *Mol. Microbiol.* **46**:869–878.
64. Tu, B. P., and J. S. Weissman. 2004. Oxidative protein folding in eukaryotes: mechanisms and consequences. *J. Cell Biol.* **164**:341–346.
65. Vergés, E., N. Colomina, E. Garí, C. Gallego, and M. Aldea. 2007. Cyclin Cln3 is retained at the ER and released by the J chaperone Ydj1 in late G1 to trigger cell cycle entry. *Mol. Cell* **26**:649–662.
66. Wach, A., A. Brachat, R. Pöhlmann, and P. Philippsen. 1994. New heterologous modules for classical or PCR-based gene disruptions in *Saccharomyces cerevisiae*. *Yeast* **13**:1793–1808.
67. Weiner, M. P., and G. L. Costa. 1995. Rapid PCR site-directed mutagenesis, p. 613–621. In C. W. Dieffenbach and G. S. Dveksler (ed.), *PCR primer: a laboratory manual*. Cold Spring Harbor Laboratory Press, Cold Spring Harbor, NY.
68. Wingert, R. A., J. L. Galloway, B. Barut, H. Foott, P. Fraenkel, J. L. Axe, G. J. Weber, K. Dooley, A. J. Davidson, B. Schmidt, B. H. Paw, G. C. Shaw, P. Kigsley, J. Palis, H. Schubert, O. Chen, J. Kaplan, the Tübingen 2000 Screen Consortium, and L. I. Zon. 2005. Deficiency of glutaredoxin 5 reveals Fe-S clusters are required for vertebrate haem synthesis. *Nature* **436**:1035–1039.
69. Xiao, R., J. Lundström-Ljung, A. Holmgren, and H. F. Gilbert. 2005. Catalysis of thiol/disulfide exchange: glutaredoxin 1 and protein disulfide isomerase use different mechanisms to enhance oxidase and reductase activities. *J. Biol. Chem.* **280**:21099–21106.
70. Yoshimoto, H., K. Saltsman, A. P. Gasch, H. X. Li, N. Ogawa, D. Botstein, P. O. Brown, and M. S. Cyert. 2002. Genome wide analysis of gene expression regulated by the calcineurin/Crz1p signaling pathway in *Saccharomyces cerevisiae*. *J. Biol. Chem.* **277**:31079–31088.